



OPEN

The investigation on shale mechanical characteristics and brittleness evaluation

Wei Lei¹, Xiangjun Liu²✉, Yi Ding², Jian Xiong² & Lixi Liang²

Rock mechanical property is significant for shale gas development and exploitation. Shale compressive strength, tensile strength, elastic deformation and so on, are necessary parameters for drilling, completion and fracturing work in shale formation. Among all these shale mechanical parameters, brittleness is a tricky and significant rock property, which has been widely used to hydraulic fracturing design. Currently, although so many works have been conducted to investigate shale brittleness, there is no precise definition of brittleness. In particular, there is no consensus on which method is the most reliable for shale brittleness evaluation. It is vital to figure out how to evaluate shale brittleness in a reliable method. Thus, this paper presents an experimental study on shale mechanical properties, analyzing mechanical features in stress strain curve, relation between mineral content and strength, mechanical parameters at varying confined stress. Based on shale mechanical characteristics and its brittle exhibition, stress strain curve from triaxial compression test is divided into 3 stages, namely, elastic stage, plastic stage and post peak stage. In combined with brittle characteristics in 3 stages of axial and radial stress–strain curves, a new brittleness index has been established for assessing shale brittleness. In order to prove the applicability of new brittleness index, its result is compared with shale failure sample after triaxial test and existing brittleness indexes based on mineral content, elastic deformation, energy, stress and strain, showing a good consistency and proving its practicability. Based on this brittleness index, influence factors of shale brittleness have been discussed. It is shown that elastic module is the most important factor of shale brittleness. Bedding plane makes shale brittleness have strong anisotropy. Brittleness is not only relied on its structure and mineral (like bedding plane, silicate and clay mineral content), but is also highly affected by external stress. Large confined pressure is able to impair shale brittleness. Outcome in this study can offer theoretical guidance for shale exploitation.

As a potential unconventional and clean resource, shale gas has attracted great attention in the whole world. Many countries have conducted their works on shale gas development^{1,2}. To efficiently explore shale gas, horizontal drilling and hydraulic fracturing are two vital technologies³. Both of these technologies are highly relied on shale mechanical property. For instance, shale compressive strength is associated with wellbore stability in drilling. Especially, shale compressive strength at the wall of borehole is an important factor for drilling design, including drilling fluid density, wellbore trajectory, wellbore configuration and so on^{4–6}. For hydraulic fracturing in shale, tensile strength and fracture toughness have huge impact on hydraulic fracture initiation and propagation, finally leading to affect the hydraulic fracturing^{7,8}. Therefore, through experimental method and numerical simulation, shale mechanical parameters have been investigated by many researchers to guide drilling and hydraulic fracturing in shale formation^{9–11}.

As one of shale mechanical properties, brittleness is a necessary factor for selection of staged fracturing and clustering. High brittleness is the prerequisite for creating effective and complex fracturing network. That is the reason why brittleness is the key parameter in fracturing stimulation. When it comes to brittleness, lots of scholars have studied on its definition, yet there is still no uniform view. All existing brittleness indexes, which have been classified into four types, i.e., methods based on mineral content, elastic deformation, energy, stress–strain, have been demonstrated in Table 1. For brittleness index (B_1) based on mineral content¹², B_1 implies that high brittle mineral content represents strong brittleness. But the limitation is that mineral content doesn't consider

¹Petroleum Engineering Technology Research Institute, SINOPEC Southwest Oil & Gas Company, Deyang 618000, Sichuan, People's Republic of China. ²State Key Laboratory of Oil and Gas Reservoir Geology and Exploitation, Southwest Petroleum University, Chengdu 610500, Sichuan, People's Republic of China. ✉email: 13880093092@163.com

Type	Evaluation methods	Variable declaration	Reference
Method based on mineral content	$B_1 = \frac{W_Q}{W_T}$	W_Q, W_T are brittle mineral weight and total mineral weight	Jarvie et al. ¹²
Method based on elastic deformation	$B_2 = \frac{E_n + \mu_n}{2}$	E_n, μ_n are normalized Young modulus and Poisson ratio	Rickman et al. ¹³
Method based on stress	$B_3 = \frac{\sigma_c}{\sigma_t}$	σ_c, σ_t are compressive strength and tensile strength	Hucka and Das ¹⁹
	$B_4 = \frac{\sigma_c - \sigma_t}{\sigma_c + \sigma_t}$		Hucka and Das ¹⁹
	$B_5 = (\sigma_t \sigma_c)^{0.5} / 2$		Altindag ¹⁴
	$B_6 = \frac{\sigma_p - \sigma_r}{\sigma_p}$	σ_p, σ_r are peak and residual strength	Bishop ¹⁵
	$B_7 = \sqrt{\sigma_T}$	σ_T is maximum tensile strength	Altindag and Guncy ¹⁶
Method based on strain	$B_8 = \frac{V_c}{V_l}$	V_c and V_l are parameters from Marinell hardness of nano-indentation method	Fan et al. ¹⁷
	$B_9 = \frac{\varepsilon_p - \varepsilon_r}{\varepsilon_p}$	$\varepsilon_p, \varepsilon_r$ are peak and residual strain	Hajia and Peter ¹⁸
Method based on energy	$B_{10} = \frac{\varepsilon_{el}}{\varepsilon_{tot}}$	$\varepsilon_{el}, \varepsilon_{tot}$ are elastic and total strain at failure, respectively	Hucka and Das ¹⁹
	$B_{11} = \frac{U^f}{U^e}$	U^f, U^e are total failure energy and consumed elastic strain energy during the failure process, respectively	Tarasov and Randolph ²⁰
	$B_{12} = \frac{U^a}{U^e}$	U^a is the additional input energy	Tarasov and Potvin ²¹
Others	$B_{13} = \frac{U^a}{U^e + U_p^d}$	U_p^d is peak dissipated energy	Ai et al. ²⁶
	$B_{14} = \frac{H}{K_{IC}}$	H is hardness and K_{IC} is fracturing toughness	Lawn and Marshall ²²
	$B_{15} = \frac{\sigma_1 - \sigma_3}{2C \cos \varphi + (\sigma_1 + \sigma_3) \sin \varphi}$	C, φ are cohesion and internal friction angle. σ_1, σ_3 are maximum and minimum principal stress	Papanastasiou et al. ²³
	$B_{16} = 0.198\sigma_c - 2.174\sigma_t + 0.913\rho - 3.807$	ρ is rock density	Yagiz ²⁴
	$B_{17} = e^{\frac{E}{10M} \times \frac{\sigma_p - \sigma_r}{\sigma_p} \times \sin \varphi}$	M is post-peak modulus, GPA	Zhou et al. ²⁵

Table 1. Brittleness evaluation methods.

external condition. Rickman et al.¹³ gives brittleness evaluation based on elastic deformation (B_2). Now, B_2 is the most widely used methods in oilfield practice. B_2 uses Young modulus and Poisson ratio to assess shale brittleness. It indicates that shale with high Young modulus and low Poisson ratio has strong brittleness. Whereas, B_2 is merely based on statistical results. In particular, elastic parameters are unable to exhibit brittle characteristic in plastic stage or post peak stage. Additionally, in fracture mechanics, brittle material is characterized by high resistance of deformation and small resistance of fracturing. Brittleness is the exhibition of shale mechanical property. Thus, based on stress strain curve that contains many rock mechanical information, numerous brittle indexes have been established. Altindag¹⁴, Bishop et al.¹⁵, Altindag and Guncy¹⁶, Fan et al.¹⁷ use shale stress (peak compressive stress and tensile stress) to establish brittle indexes ($B_3, B_4, B_5, B_6, B_7, B_8$). Even though those stress parameters are able to reflect brittleness to some extent, they are all acquired from the peak point at loading or post point after failure, which neglects brittle feature before peak point, thus probably making some errors in brittleness evaluation. Similarly, Hajia¹⁸, Hucka and Das¹⁹ use strain to build brittle indexes (B_9, B_{10}). To further obtain rock mechanical property from stress strain, brittleness indexes based on energy evolution during rock failure have been given^{20,21}. These indexes still can not express the brittleness features at the whole process of stress strain curves. Given different definitions, so far more than 20 methods have been proposed to quantify brittleness^{22–25}. Since various methods exist and depend on different theories, it is very difficult to confirm which one is more accurate. Those uncertainties inevitably cause errors in quantifying brittleness in the application.

It is clear from the literature review that numerous researches utilize various kinds of parameters to assess brittleness, but most of their studies only consider the brittle property from one aspect, lack of comprehensive analysis, which will impair its precision. Although there are lots of studies about brittleness evaluations on the basis of stress strain curve, these methods are depended on axial stress strain curve. The brittle performance not only shows up at axial deformation, but also exists in radial deformation. Therefore, it is significant to have further research on shale brittleness evaluation. In this study, shale mechanical characteristics has been acquired using triaxial test. In addition, considering brittle performance in elastic stage, plastic stage, post-peak stage at axial and radial stress–strain curve, a new brittle index has been built. According to this new brittle index, influence factors of shale brittleness have been fully discussed. The outcome of this paper can improve the understanding of shale brittleness and is meaningful for shale gas development.

Shale sample

Shale sample has been acquired from Longmaxi formation, Sichuan basin (depth is located at 4390–4420 m). SEM test illustrates shale of Longmaxi formation is rich with microfractures and micropores, shown as Fig. 1a. According to XRD test results (Fig. 1b), clay and quartz are dominated in shale, with 34.6% and 40.5% average content. Also, brittle minerals, such as quartz, potash feldspar and plagioclase, are over 50% of mineral content, showing strong brittleness of shale.

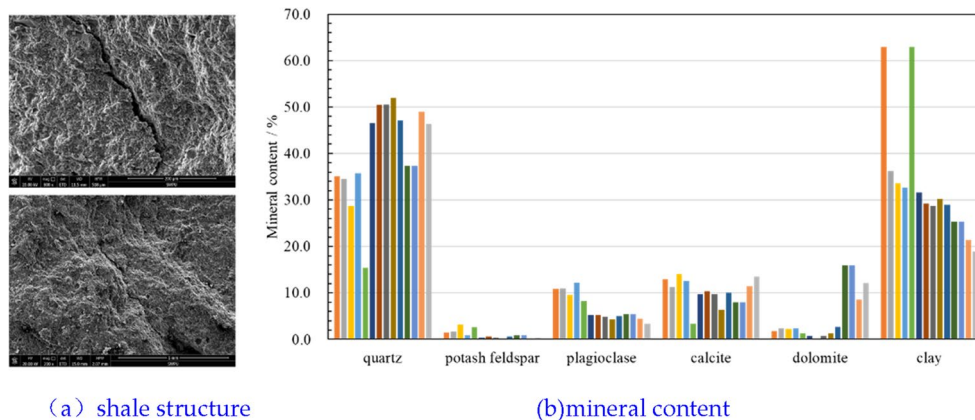


Figure 1. Shale micro-structure and mineral content.

No	Depth/m	Length/mm	Diameter/mm	Density/g cm ³	Porosity/%	P wave/ μ s ft	S wave/ μ s ft
1	4388.68	50.63	24.96	2.66	3.8	193.56	333.40
2	4392.69	50.54	25.05	2.65	1.8	199.85	332.43
3	4396.45	50.39	25.06	2.64	2.17	203.20	338.14
4	4396.71	50.32	25.04	2.64	1.38	197.77	335.06
5	4397.60	50.30	25.08	2.65	3.82	197.61	334.00
6	4403.14	50.58	25.18	2.56	1.22	203.64	336.10
7	4407.25	50.57	25.24	2.56	6.39	201.29	335.35
8	4408.91	50.15	25.20	2.55	2.30	201.79	335.00
9	4409.88	50.06	25.14	2.53	4.69	204.97	337.22
10	4412.35	50.20	25.10	2.54	2.67	207.58	334.68
11	4412.41	50.31	25.09	2.55	2.76	201.56	343.49
12	4414.67	50.20	25.15	2.53	7.51	202.78	350.57
13	4415.41	50.37	25.22	2.53	2.55	205.68	354.18
14	4416.63	50.21	25.16	2.53	1.91	200.35	345.72

Table 2. Rock physical property of shale sample.

In addition, core samples have been used for rock physical test, including density, acoustic property, porosity, etc., shown as Table 2. Density and porosity of shale are 2.53–2.66 g/cm³ and 1.21–7.51% respectively. Interval transit time of P wave and S wave are 193.56–207.58 us/ft and 332.43–354.18 us/ft. Based on rock physical property of shale, samples are selected and prepared for following triaxial test.

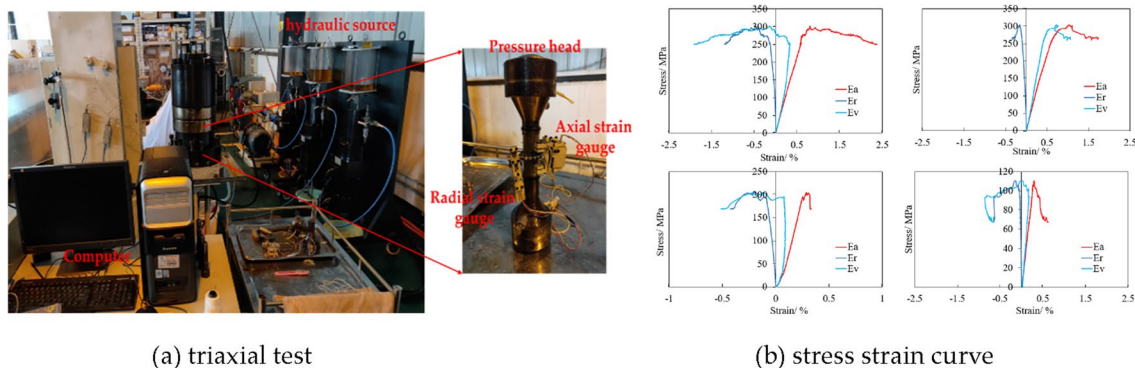


Figure 2. Triaxial test and its stress strain curve of shale.

Shale mechanical characteristics

Triaxial test

In this paper, shale mechanical characteristics is exhibited by conducting triaxial test, shown as Fig. 2a. Based on that, stress strain curves with certain confined stress have been acquired, shown as Fig. 2b. Stress strain curve is able to give mechanical parameters, such as compressive strength (peak stress), elastic module, Poisson ratio, which are all indicators of shale rock mechanical characteristics.

Relation between mineral content and mechanical parameters

In order to obtain the association between mineral content and mechanical parameters, triaxial test and XRD have been combined. After triaxial test, shale fragments were collected for mineral content analysis. Results are shown as Fig. 3. Minerals are classified to 3 types, which are silicate (quartz, potash feldspar, plagioclase), calcium (calcite, dolomite) and clay mineral. It can be found that compressive strength has decline with increasing silicate and calcium mineral since they (quartz, potash feldspar) are comparatively strong strength mineral. On the other hand, clay as relatively lower strength mineral, is adverse to shale strength. Since silicate mineral is brittle mineral, high content of silicate mineral leads to large elastic module and small Poisson ratio, which are typical brittle features according to Rickman¹³. In contrast, clay normally has plastic property. Its increasing content causes small elastic module and large Poisson ratio.

Influence of confined stress on shale mechanical characteristics

To further analyze shale mechanical characteristics in different stress conditions, triaxial tests with various confined pressures have been conducted, and its result is shown in Fig. 4. Furthermore, based on stress strain curves with different confined pressures, compressive strength, elastic module and Poisson ratio have been illustrated in Fig. 5. It is shown that confined pressure can increase compressive strength because it adds up lateral braced force. With rising confined pressure, elastic module has growing trend and no clear change of Poisson ration is noticed.

Influence of bedding plane on shale mechanical characteristics

Shale is typical laminated material with parallel bedding plane, which normally has weak strength¹⁰. In order to analyze the influence of weak plane on shale mechanical property, shale samples with variable bedding plane angles have been applied to triaxial test. Results are shown as Fig. 6. With increasing bedding plane angle, shale strength and elastic module firstly decline and reach lowest point at approximately 55°. Then, shale strength

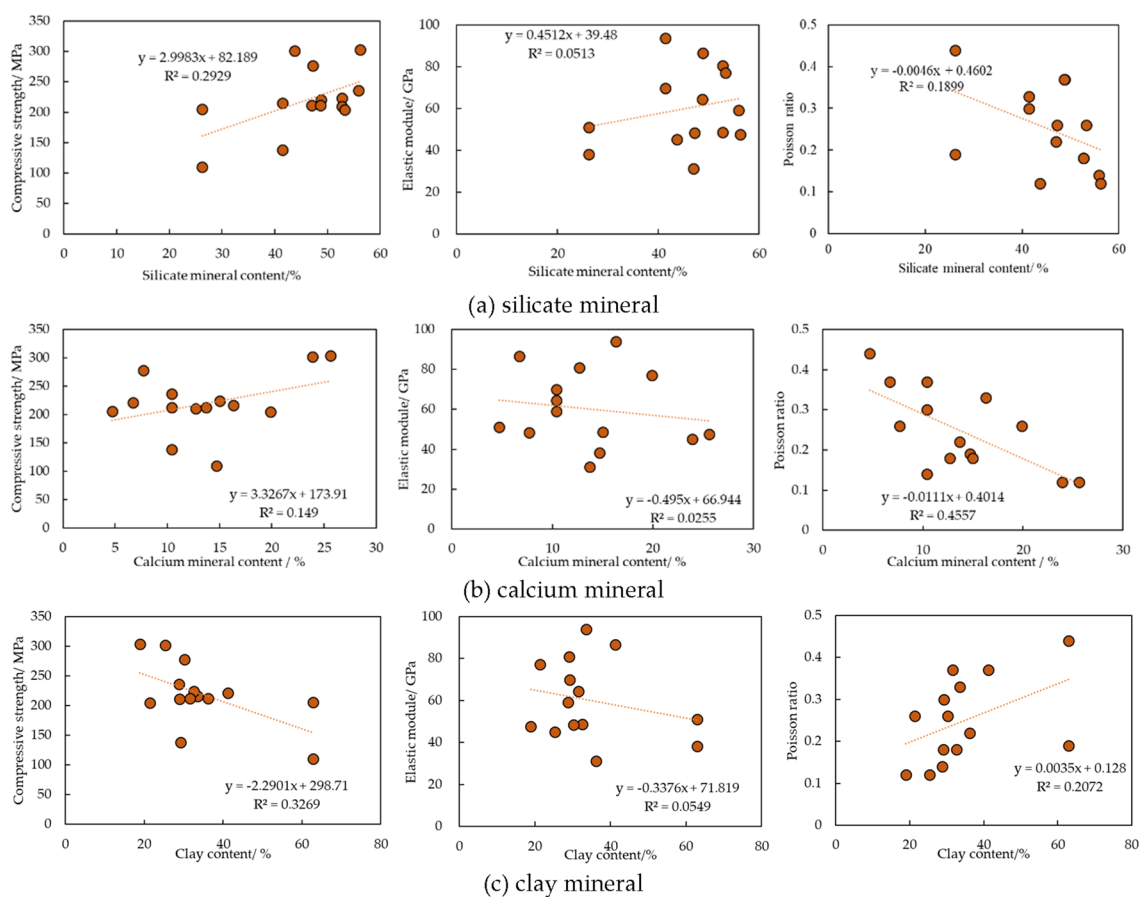


Figure 3. Relation between mineral content and mechanical parameters.

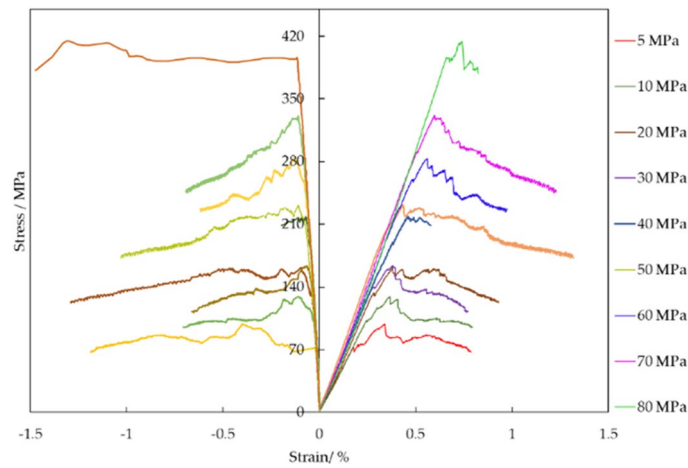


Figure 4. Stress strain curves with different confined pressure.

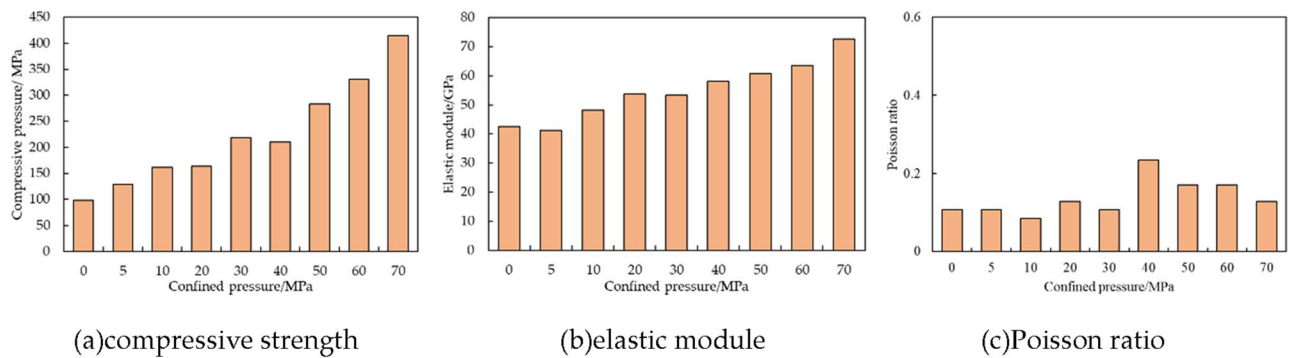


Figure 5. Shale rock mechanical parameters with different confined pressure.

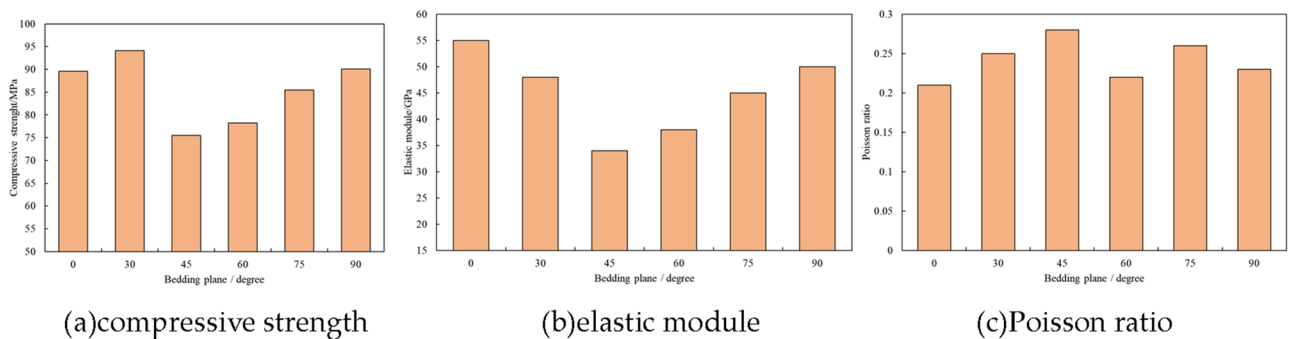


Figure 6. Shale rock mechanical parameters with different bedding plane angles.

and elastic module rise back to original value. In contrast, varying bedding plane angles have little impact on Poisson ratio.

Shale brittleness

New brittleness index based on stress strain curve

It has been known that brittleness is largely relied on stress strain curve. Correspondingly, many brittleness indexes have been established based on stress strain curve²⁷. However, few evaluation methods can cover the whole process of stress strain curve, mainly focus on elastic stage or post-peak stage. Brittleness is exhibited in the overall process of rock failure, thus evaluation based on whole process of stress strain curve is necessary. In addition, most of brittle evaluations are built on axial stress–strain curve, ignoring the radial stress–strain curve that is an important indicator of rock brittleness.

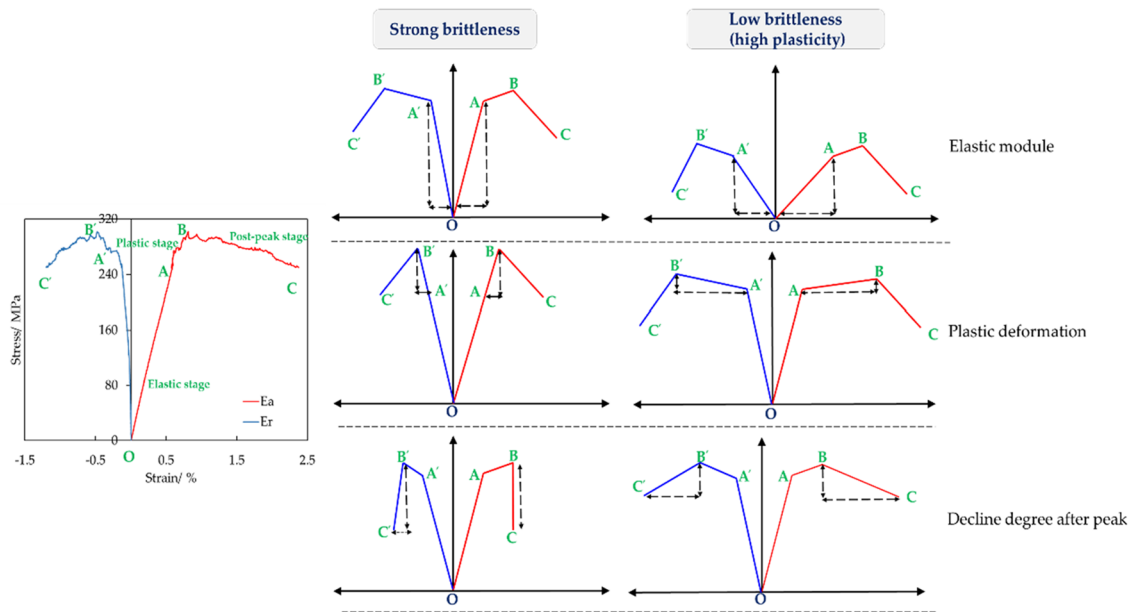


Figure 7. Schematic of shale brittleness index.

According to rock mechanical theory and existing brittleness evaluation, typical brittle characteristics in stress strain curves are listed as^{28–30}: (1) few elastic deformation (large elastic module), (2) plastic stage is short; (3) stress has dramatic dropping after peak point; (4) small ratio of radial to axial deformation. All these features are in stress strain curve shown as Fig. 7. Based on Fig. 7, for axial and radial stress–strain curve, they all can be divided into 3 stages, i.e., elastic stage, plastic stage and post-peak stage. Based on above brittle characteristics, angles of inclination of stress–strain curves in each stage have been applied to build brittle index, shown as:

$$\begin{cases} BI_a = \arctan \frac{\sigma_A}{\varepsilon_A} + \arctan \frac{\sigma_B - \sigma_A}{\varepsilon_B - \varepsilon_A} + 180^\circ - \arctan \frac{\varepsilon_C - \varepsilon_B}{\sigma_B - \sigma_C} \\ BI_r = \arctan \frac{\sigma_{A'}}{-\varepsilon_{A'}} + \arctan \frac{\sigma_{B'} - \sigma_{A'}}{\varepsilon_{A'} - \varepsilon_{B'}} + 180^\circ - \arctan \frac{\varepsilon_{C'} - \varepsilon_{B'}}{\sigma_{C'} - \sigma_{B'}} \end{cases} \quad (1)$$

where BI_a , BI_r are brittle indexes based on axial stress–strain curve and radial stress–strain curve. σ_A and ε_A are stress and strain at point A. σ_B and ε_B are stress and strain at point B. σ_C and ε_C are stress and strain at point C. $\sigma_{A'}$ and $\varepsilon_{A'}$ are stress and strain at point A'. $\sigma_{B'}$ and $\varepsilon_{B'}$ are stress and strain at point B'. $\sigma_{C'}$ and $\varepsilon_{C'}$ are stress and strain at point C'.

In addition, small ratio of radial to axial deformation represents high brittleness, thus giving a brittle index:

$$BI_{ar} = \left| \frac{\sigma_A/\varepsilon_A}{\sigma_{A'}/\varepsilon_{A'}} \right| \quad (2)$$

In combination with Eq. (1) and Eq. (2), a new brittleness index including all brittle characteristics in stress strain curves has been established, shown as:

$$BI = \frac{1}{3} \left(\frac{BI_a - BI_{a \min}}{BI_{a \max} - BI_{a \min}} + \frac{BI_r \max - BI_r}{BI_r \max - BI_r \min} + \frac{BI_{ar} - BI_{ar \min}}{BI_{ar \max} - BI_{ar \min}} \right) \quad (3)$$

where BI is final brittleness index. $BI_{a \max}$, $BI_{a \min}$ are maximum and minimum BI_a . $BI_r \max$, $BI_r \min$ is maximum and minimum BI_r . $BI_{ar \max}$, $BI_{ar \min}$ are maximum and minimum BI_{ar} .

Verification of new brittleness index

In order to verify this brittleness index, two comparisons have been done. Firstly, rock with high brittleness indicates strong damaging degree after failure, which is also the reason why brittleness is an important factor of hydraulic fracturing^{31–33}. Classifications based on failure degree of shale sample and BI have been illustrated respectively in Fig. 8. Secondly, existing brittleness methods, which are established on mineral content (BI_f), elastic deformation (BI_2), stress (BI_6), strain (BI_8) and energy (BI_{12}) respectively, have been selected. The relation between BI and existing brittleness methods have been given, shown as Fig. 9.

It is shown that brittleness classification based on BI accords with failure degree of shale sample (Fig. 8d). Samples with multiple cracks and strong degree of fragmentation after triaxial test show high value of BI . Besides, samples with single crack and low degree of fragmentation have small value of BI . This consistency proves BI has a good ability of brittleness prediction. Additionally, BI is consistency with five types of existing brittleness (Fig. 9), further proving the accuracy of BI .

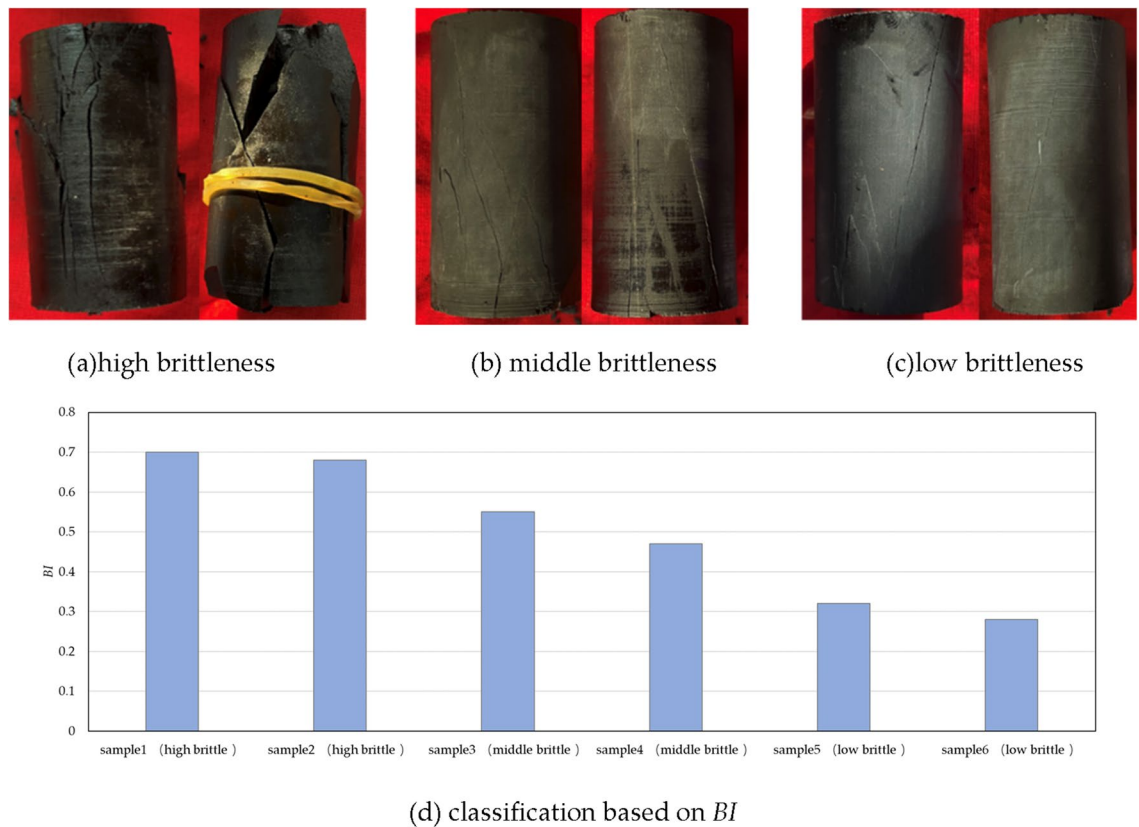


Figure 8. Brittleness classification of shale in Longmaxi reservoir.

Influence factors of shale brittleness

In the oilfield, shale brittleness is evaluated on the logging data, which can not directly give shale stress strain curve. Thus, it is necessary to establish shale brittleness evaluation based on parameters from logging, such as mineral distribution, density, interval transit time (DT), porosity, elastic module, Poisson ratio, confined pressure and bedding plane occurrence³⁴. Therefore, in this part, relation between these influence factors and shale brittleness has been discussed.

First of all, the fundamental logging information are rock physical, such as acoustic interval transit time (DT), density and porosity. Their correlations with shale brittleness are shown as Fig. 10. Shale brittleness has no association with these rock physical parameters, meaning that it is unable to evaluate shale brittleness by using these basic logging data.

In addition, based on sonic wave theory, elastic parameters (elastic module and Poisson ratio) can be acquired using DT and density. Correspondingly, their relations with brittleness have been illustrated in Fig. 11. It is found that with increasing brittleness, elastic module grows and Poisson ratio decreases. This pattern further proves the practicability of Rickman equation and also indicates that elastic parameters are robust factors of evaluating shale brittleness.

Logging is able to offer profile of mineral content. The relation between mineral content and brittleness is shown in Fig. 12. It demonstrates that silicate and calcium, as typical brittle mineral, are beneficial for shale brittleness. On the other hand, with increasing clay that has small brittleness, shale brittleness shows decline. Results indicate that mineral content is an important factor of shale brittleness.

Bedding plane is a significant structure that can affect rock mechanics. The association between bedding plane occurrence and brittleness is shown in Fig. 13. It is shown that brittleness firstly increases and then drops with rising bedding plane angle. It can be explained by the failure model of shale. Bedding plane is the typical weak strength plane. In this condition, when axial stress acts on shale, it is likely to have failure along bedding plane. With shale failure along bedding plane, its strength is small. Axial stress can cause stronger and fast structural damage, thus expressing high brittleness. Furthermore, shale brittleness is not depended on its physical, mechanical property, mineral content and structure, it is also affected by external stress. Therefore, relation between confined pressure and brittleness has been illustrated in Fig. 14. Since confined pressure has restriction on strain and boost impact on strength, meaning that it is not easy to create crack and make sample failure during mechanical test. Thus, this small failure degree express low brittleness.

According to above analysis, elastics module, Poisson ratio, silicate content, calcium content, clay content, bedding plane angle and confined pressure are all important influence factors of shale brittleness. In order to quantify the importance degree of all influence factors, normalization processing has been applied to all influence factors, shown as:

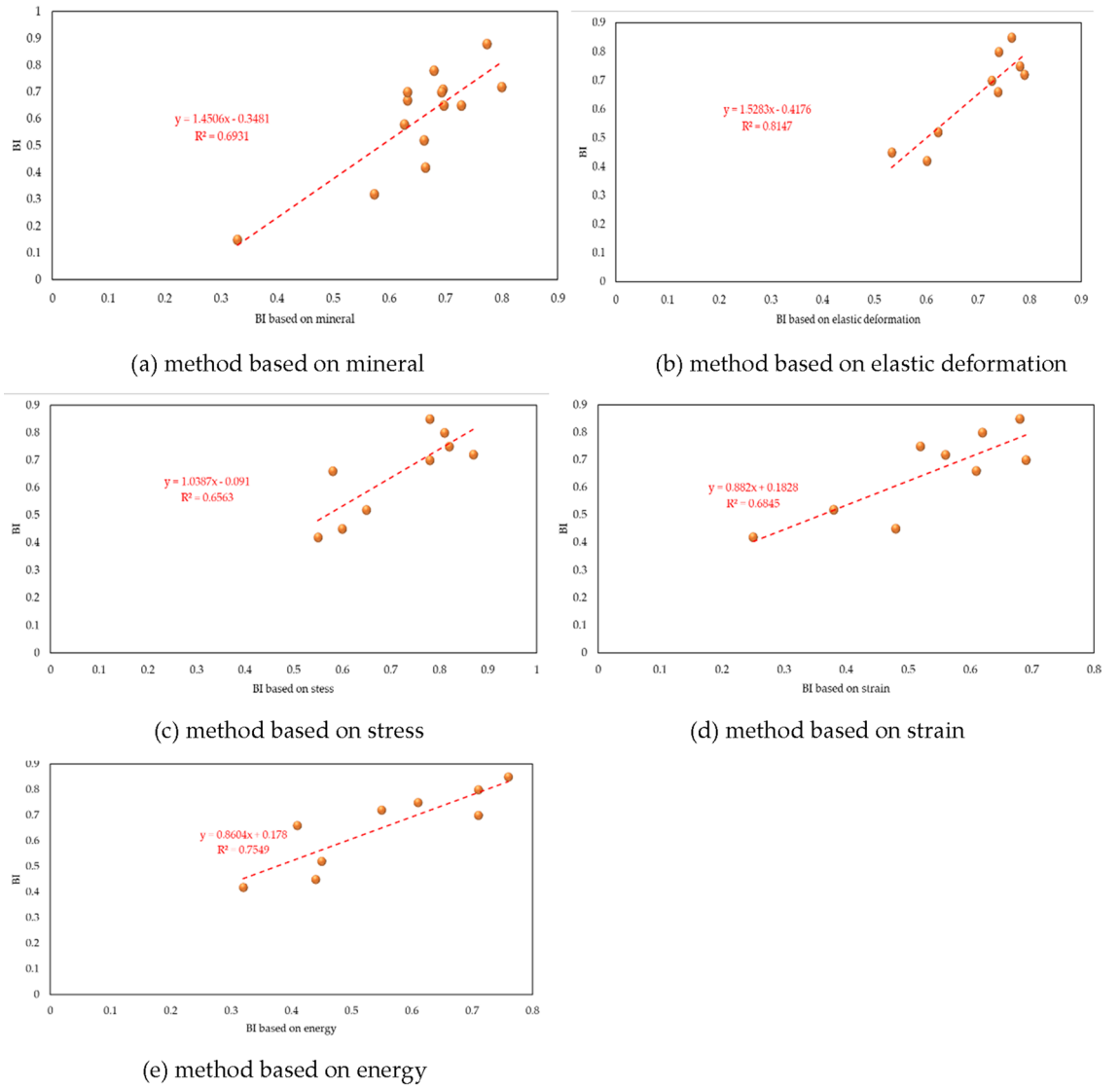


Figure 9. Relation of *BI* and existing brittleness method.

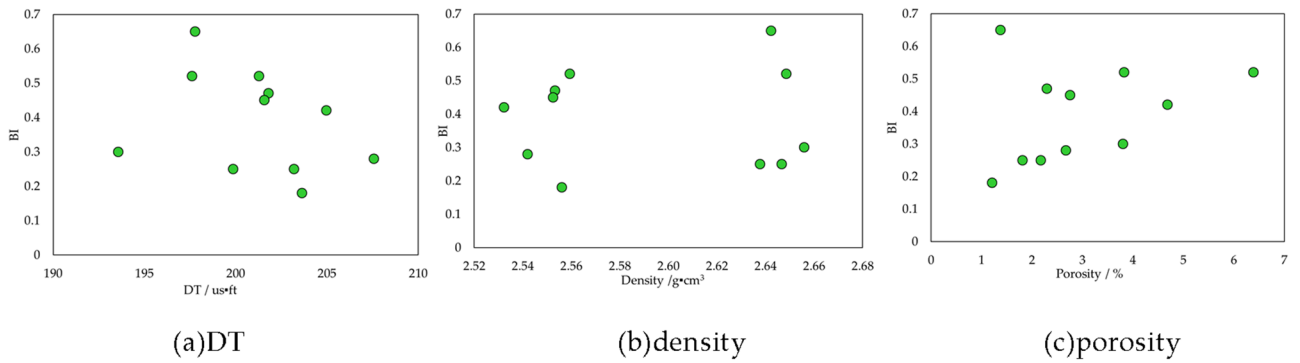


Figure 10. Relation of *BI* and shale physical properties.

$$\begin{cases} Y(i) = \frac{x(i) - X_{\min}(i)}{X_{\max}(i) - X_{\min}(i)} & \text{positive correlation} \\ Y(i) = \frac{X_{\max}(i) - x(i)}{X_{\max}(i) - X_{\min}(i)} & \text{negative correlation} \end{cases} \quad i = 1, 2, 3, \dots, n \quad (4)$$

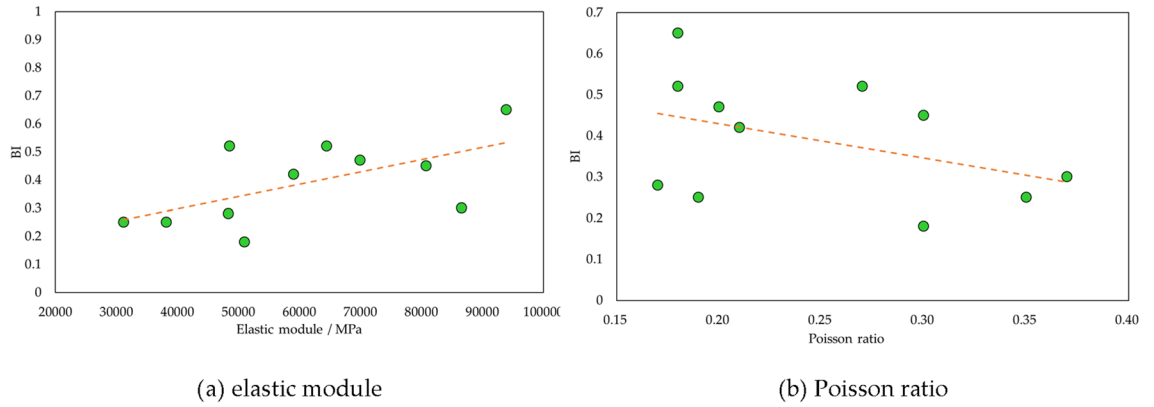


Figure 11. Relation of *BI* and elastic module, Poisson ratio.

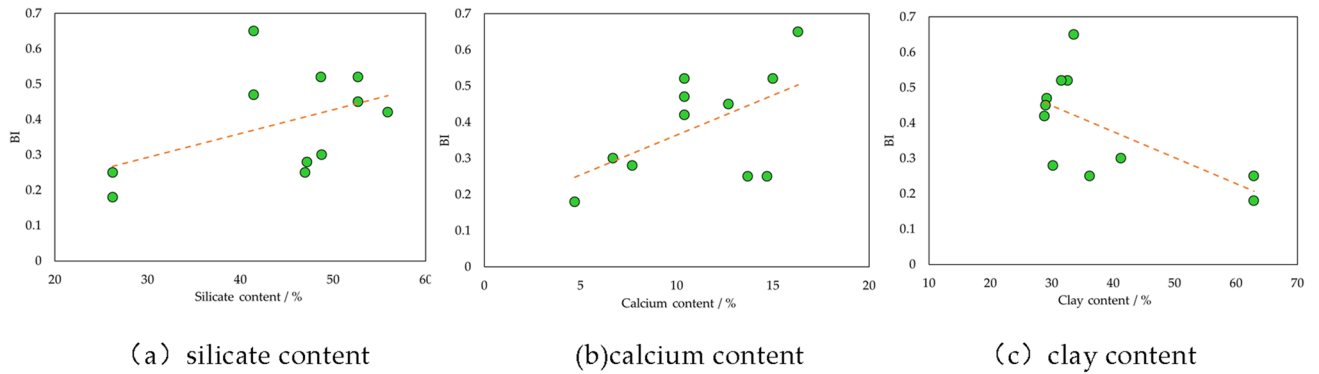


Figure 12. Relation of *BI* and mineral content.

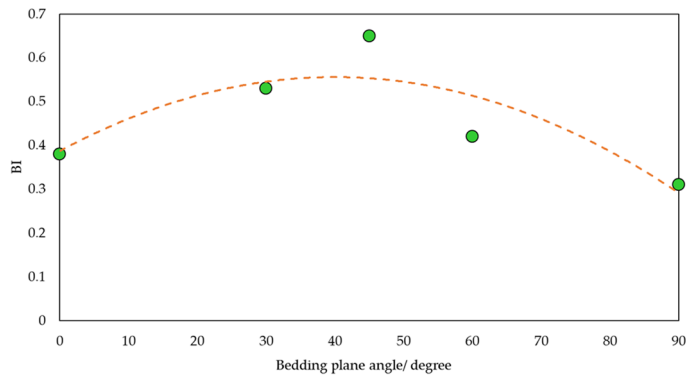


Figure 13. Relation of *BI* and bedding plane.

where $x(i)$ is value of influence factor. $X_{\max}(i)$, $X_{\min}(i)$ are maximum and minimum $x(i)$ $Y(i)$ is normalization of $x(i)$.

After normalization, changing coefficient of influence factor i ($Z(i)$) has been obtained :

$$Z(i) = \frac{BI_{\max}(i) - BI_{\min}(i)}{Y(i)_{\max} - Y(i)_{\min}} \tag{5}$$

where $BI_{\max}(i)$, $BI_{\min}(i)$ are maximum and minimum brittleness index with changing $Y(i)$. $Y(i)_{\max}$, $Y(i)_{\min}$ are value of $Y(i)$ when brittleness indexes are maximum and minimum respectively.

Obviously, larger $Z(i)$ indicates that influence factor i ($x(i)$) has stronger impact on brittleness index. Hence, based on $Z(i)$, weight coefficients of all influence factors are computed using Eq. (6), illustrated as Fig. 15.

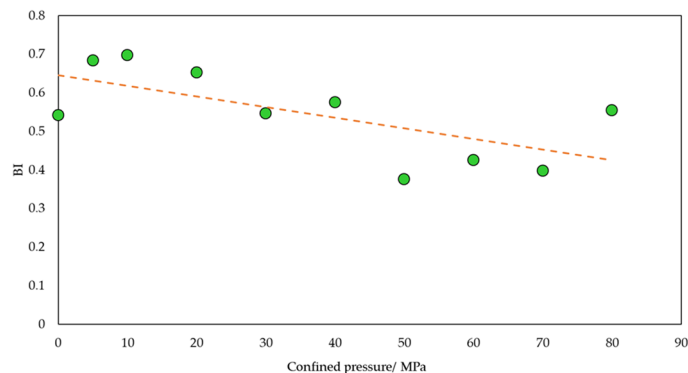


Figure 14. Relation of *BI* and confined pressure.

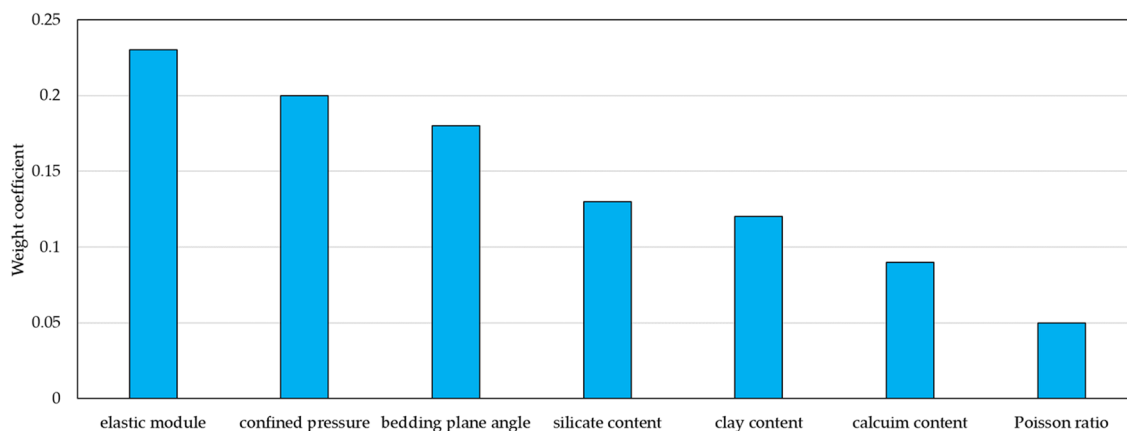


Figure 15. Weight coefficients of all influence factors of shale brittleness.

$$\delta(i) = \frac{Z(i)}{\sum_{i=1}^n Z(i)} \quad i = 1, 2, 3, \dots, n \quad (6)$$

It is shown that elastic module has highest weight coefficients, but the influence of Poisson ratio is smallest. Mineral content plays a big role in shale brittleness. In particular, silicate and clay mineral content are directly linked to brittleness. Weight coefficient of confined pressure is large, indicating external condition is vital for shale brittleness evaluation. Also, it indicates shale brittleness has decline when shale gas exploitation goes into deep shale formation with high stress. Due to rich bedding plane, shale has strong anisotropy in brittleness. Since weight coefficient of bedding plane angle is so high, it is necessary to consider bedding plane occurrence in shale brittleness evaluation.

Application

This new brittleness index has been applied into shale formation of W4 well. Core samples have been taken from W4 well. Thus, brittleness indexes at location of core samples have been calculated using this new index, shown as Fig. 16. It is shown that brittleness index at 4000–4050 m depth is relatively higher than that index at 4080–4100 m depth. Average brittleness index is 0.56 at 4000–4050 m depth. In contrast, at 4080–4100 m depth, brittleness index is merely 0.33. According to hydraulic fracturing fracture from micro-seismic monitoring, fracture volume at 4000–4050 m depth is larger than that at 4080–4100 m depth, proving the practicability of brittleness index.

Conclusion

- (1) Shale mechanical characteristics have been fully analyzed. Compressive strength has decline with increasing silicate and calcium mineral since quartz, potash feldspar are comparatively strong strength mineral. On the other hand, clay, as relatively lower strength mineral, is adverse to shale strength. Also, high content of silicate mineral lead to large elastic module and small Poisson ratio. In contrast, clay normally has plastic property. Its increasing content lead to small module and large Poisson ratio. Confined pressure can increase

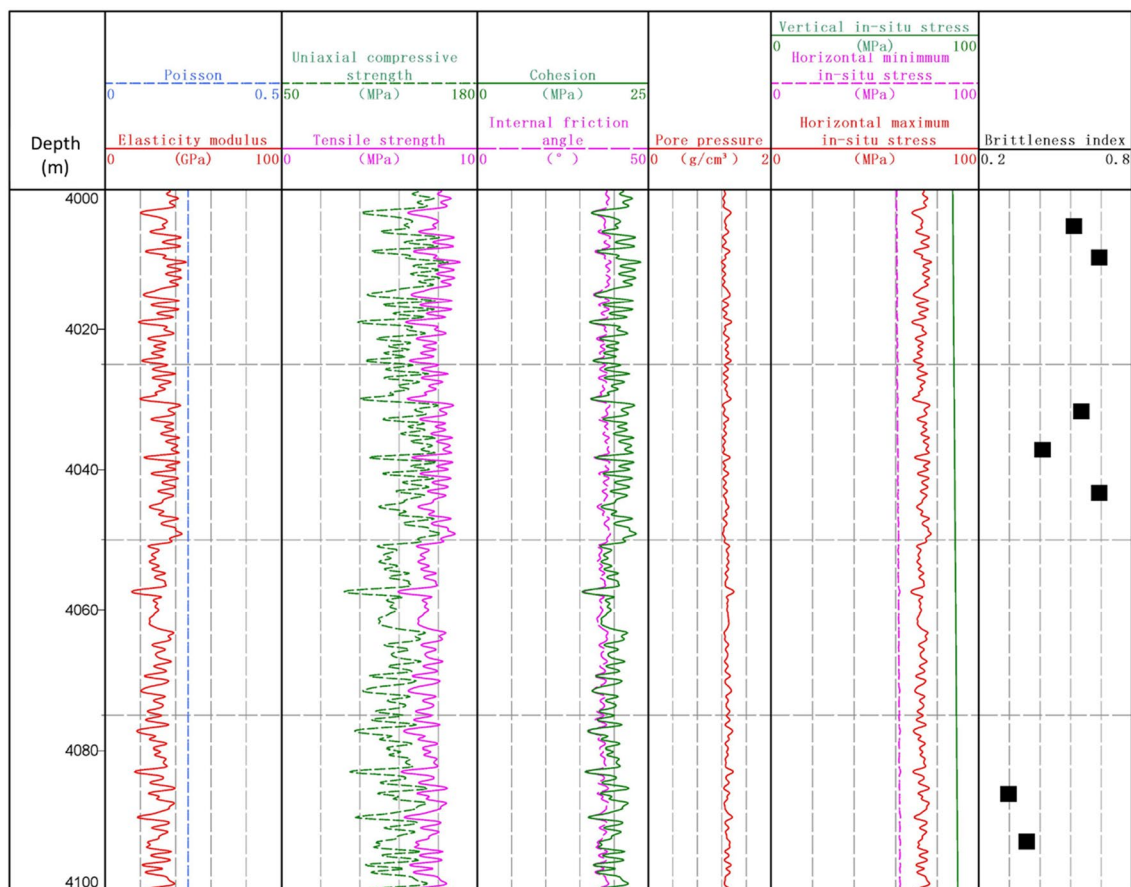


Figure 16. Brittleness index of W4 well.

- compressive strength because it adds up lateral braced force. With increasing bedding plane angle, shale strength will have decline at approximately 55°.
- (2) A new shale brittleness index has been established based on fully axial and radial stress–strain curve in elastic, plastic and post-peak stage. Its accuracy has been proved by shale failure degree and its correlation with existing brittleness evaluation method.
 - (3) Based on the changing coefficient of all influence factors, important degree of factors have been analyzed. Elastic module has highest weight coefficients. Mineral content plays a big role in shale brittleness. Weight coefficient of confined pressure is large, indicating external condition is vital for shale brittleness evaluation. Rich bedding plane gives shale strong anisotropy in brittleness. Thus, large weight coefficient of bedding plane angle suggests that bedding plane occurrence has to be considered in shale brittleness evaluation.

Data availability

The datasets generated and/or analysed during the current study are not publicly available due to requirement of confidentiality, but are available from the corresponding author on reasonable request.

Received: 22 May 2023; Accepted: 13 December 2023

Published online: 22 December 2023

References

1. Wang, Q. *et al.* Natural gas from shale formation—the evolution, evidences and challenges of shale gas revolution in United States. *Renew. Sustain. Energy Rev.* **30**, 1–28 (2014).
2. Rivard, C. *et al.* An overview of Canadian shale gas production and environmental concerns. *Int. J. Coal Geol.* **126**, 64–76 (2014).
3. Vengosh, A. *et al.* A critical review of the risks to water resources from unconventional shale gas development and hydraulic fracturing in the United States. *Environ. Sci. Technol.* **48**(15), 8334–8348 (2014).
4. Guo, B. *et al.* The maximum permissible fracturing pressure in shale gas wells for wellbore cement sheath integrity. *J. Nat. Gas Sci. Eng.* **56**, 324–332 (2018).
5. Zhao, C. *et al.* Analysis of well stress with the effect of natural fracture nearby wellbore during hydraulic fracturing in shale gas wells. *J. Petrol. Sci. Eng.* **188**, 106885 (2020).
6. Liang, C. *et al.* Wellbore stability model for shale gas reservoir considering the coupling of multi-weakness planes and porous flow. *J. Nat. Gas Sci. Eng.* **21**, 364–378 (2014).

7. Vengosh, A. *et al.* The effects of shale gas exploration and hydraulic fracturing on the quality of water resources in the United States. *Procedia Earth Planet. Sci.* **7**, 863–866 (2013).
8. Kim, J. & Moridis, G. J. Numerical analysis of fracture propagation during hydraulic fracturing operations in shale gas systems. *Int. J. Rock Mech. Min. Sci.* **76**, 127–137 (2015).
9. Sone, H. & Zoback, M. D. Mechanical properties of shale-gas reservoir rocks—Part 1: Static and dynamic elastic properties and anisotropy. *Geophysics* **78**(5), 381–392 (2013).
10. Heng, S. *et al.* Experimental study on the mechanical properties of bedding planes in shale. *J. Nat. Gas Sci. Eng.* **76**, 103161 (2020).
11. Labani, M. M. & Rezaee, R. The importance of geochemical parameters and shale composition on rock mechanical properties of gas shale reservoirs: A case study from the Kockatea Shale and Carynginia Formation from the Perth Basin, Western Australia. *Rock Mech. Rock Eng.* **48**(3), 1249–1257 (2015).
12. Jarvie, D. M. *et al.* Unconventional shale-gas systems: The Mississippian Barnett Shale of north-central Texas as one model for thermogenic shale-gas assessment. *AAPG Bull.* **91**(4), 475–499 (2007).
13. Rickman, R., Mullen, M. J., Petre, J. E., *et al.* A practical use of shale petrophysics for stimulation design optimization: All shale plays are not clones of the Barnett Shale. In SPE Annual Technical Conference and Exhibition. OnePetro (2008).
14. Altindag, R. Correlation of specific energy with rock brittleness concepts on rock cutting. *J. Southern Afr. Inst. Min. Metall.* **103**(3), 163–171 (2003).
15. Bishop, A. W. *et al.* A new ring shear apparatus and its application to the measurement of residual strength. *Geotechnique* **21**(4), 273–328 (1971).
16. Altindag, R. & Guney, A. Predicting the relationships between brittleness and mechanical properties (UCS, TS and SH) of rocks. *Sci. Res. Essays* **5**(16), 2107–2188 (2010).
17. Fan, X. *et al.* Brittleness evaluation of the inter-salt shale oil reservoir in Jiangnan Basin in China. *Mar. Pet. Geol.* **102**, 109–115 (2019).
18. Hajiabdolmajid, V. & Kaiser, P. Brittleness of rock and stability assessment in hard rock tunneling. *Tunnell. Underground Space Technol.* **18**(1), 35–48 (2003).
19. Hucka, V. & Das, B. Brittleness determination of rocks by different methods. *Int. J. Rock Mech. Min. Sci. Geomech. Abstr. Pergamon* **11**(10), 389–392 (1974).
20. Tarasov, B. G. & Randolph, M. F. Superbrittleness of rocks and earthquake activity. *Int. J. Rock Mech. Min. Sci.* **48**(6), 888–898 (2011).
21. Tarasov, B. & Potvin, Y. Universal criteria for rock brittleness estimation under triaxial compression. *Int. J. Rock Mech. Min. Sci.* **59**, 57–69 (2013).
22. Lawn, B. R. & Marshall, D. B. Hardness, toughness, and brittleness: an indentation analysis. *J. Am. Ceram. Soc.* **62**(7–8), 347–350 (1979).
23. Papanastasiou, P., & Atkinson, C. The brittleness index in hydraulic fracturing. In *49th US Rock Mechanics/Geomechanics Symposium*. OnePetro, 2015.
24. Yagiz, S. Assessment of brittleness using rock strength and density with punch penetration test. *Tunnell. Underground Space Technol.* **24**(1), 66–74 (2009).
25. Zhou, H. *et al.* A new rock brittleness evaluation index based on the internal friction angle and class i stress–strain curve. *Rock Mech. Rock Eng* **51**(7), 2309–2316 (2018).
26. Ai, C. *et al.* Estimation criteria for rock brittleness based on energy analysis during the rupturing process. *Rock Mech. Rock Eng.* **49**, 4681–4698 (2016).
27. Li, H. Research progress on evaluation methods and factors influencing shale brittleness: A review. *Energy Rep.* **8**, 4344–4358 (2022).
28. Zhang, D., Ranjith, P. G. & Perera, M. S. A. The brittleness indices used in rock mechanics and their application in shale hydraulic fracturing: A review. *J. Pet. Sci. Eng.* **143**, 158–170 (2016).
29. Kivi, I. R., Ameri, M. & Molladavoodi, H. Shale brittleness evaluation based on energy balance analysis of stress-strain curves. *J. Pet. Sci. Eng.* **167**, 1–19 (2018).
30. Meng, F., Wong, L. N. Y. & Zhou, H. Rock brittleness indices and their applications to different fields of rock engineering: a review. *J. Rock Mech. Geotech. Eng.* **13**(1), 221–247 (2021).
31. Guo, J. C. *et al.* A new method for shale brittleness evaluation. *Environ. Earth Sci.* **73**(10), 5855–5865 (2015).
32. Rybacki, E., Meier, T. & Dresen, G. What controls the mechanical properties of shale rocks?—Part II: Brittleness. *J. Pet. Sci. Eng.* **144**, 39–58 (2016).
33. Shimizu, H. *et al.* A study of the effect of brittleness on hydraulic fracture complexity using a flow-coupled discrete element method. *J. Pet. Sci. Eng.* **160**, 1 (2017).
34. Holt, R. M. *et al.* Comparing mechanical and ultrasonic behaviour of a brittle and a ductile shale: Relevance to prediction of borehole stability and verification of shale barriers. *J. Pet. Sci. Eng.* **187**, 106746 (2019).

Acknowledgements

This work was supported by the National Natural Science Foundation of China (Nos. 42202194, and 51274172). We appreciate their support.

Author contributions

W.L.: Resources, Funding acquisition, Validation, Writing; X.L.: Methodology, Conceptualization, Funding acquisition; Y.D.: Writing, Validation, Formal analysis; J.X.: Data Curation; L.L.: Resources, Funding acquisition.

Competing interests

The authors declare no competing interests.

Additional information

Correspondence and requests for materials should be addressed to X.L.

Reprints and permissions information is available at www.nature.com/reprints.

Publisher's note Springer Nature remains neutral with regard to jurisdictional claims in published maps and institutional affiliations.



Open Access This article is licensed under a Creative Commons Attribution 4.0 International License, which permits use, sharing, adaptation, distribution and reproduction in any medium or format, as long as you give appropriate credit to the original author(s) and the source, provide a link to the Creative Commons licence, and indicate if changes were made. The images or other third party material in this article are included in the article's Creative Commons licence, unless indicated otherwise in a credit line to the material. If material is not included in the article's Creative Commons licence and your intended use is not permitted by statutory regulation or exceeds the permitted use, you will need to obtain permission directly from the copyright holder. To view a copy of this licence, visit <http://creativecommons.org/licenses/by/4.0/>.

© The Author(s) 2023